Monthly Notices
of the
ROYAL ASTRONOMICAL SOCIETY

MNRAS **454,** 1517–1524 (2015) doi:10.1093/mnras/stv1885

Constraints on the distribution of supernova remnants with Galactocentric radius

D. A. Green★

Astrophysics Group, Cavendish Laboratory, 19 J. J. Thomson Avenue, Cambridge CB3 0HE, UK

Accepted 2015 August 12. Received 2015 August 5; in original form 2015 July 08

ABSTRACT

Supernova remnants (SNRs) in the Galaxy are an important source of energy injection into the interstellar medium, and also of cosmic rays. Currently there are 294 known SNRs in the Galaxy, and their distribution with Galactocentric radius is of interest for various studies. Here I discuss some of the statistics of Galactic SNRs, including the observational selection effects that apply, and difficulties in obtaining distances for individual remnants from the 'Σ–D' relation. Comparison of the observed Galactic longitude distribution of a sample of bright Galactic SNRs – which are not strongly affected by selection effects – with those expected from models is used to constrain the Galactic distribution of SNRs. The best-fitting power-law/exponential model is more concentrated towards the Galactic Centre than the widely used distribution obtained by Case & Bhattacharya.

Key words: ISM: structure – ISM: supernova remnants – Galaxy: structure.

1 INTRODUCTION

There are currently 294 supernova remnants (SNRs) known in the Galaxy (Green 2014a). These are an important source of the injection of energy and heavy elements into the interstellar medium, and are believed to be the site of acceleration of cosmic rays, at least up to 10^{15} eV (e.g. Bell 2014). Consequently, the distribution of SNRs in the Galaxy is of interest for a variety of studies of the Galaxy (e.g. Lee et al. 2011; Vladimirov et al. 2012; Kumar & Eichler 2014; Calore, Cholis & Weniger 2015).

It is not straightforward to construct a Galactic distribution directly from properties of catalogued SNRs. This is not only because distances are not available for most Galactic SNRs, but also because of the observational selection effects that apply to the current catalogue of SNRs. It is expected (Li et al. 2011) that most SNRs are from massive stars (i.e. types II/Ib/Ic), which also produce pulsars, and hence the distribution of SNRs will be closely related to that of star-forming regions or pulsars.

Some statistics of the current Galactic SNR catalogue, the selection effects that apply to their identification, and issues related to the derivation of distances to individual SNRs from the 'Σ–D' relation are discussed in Section 2. Section 3 presents constraints on the Galactic distribution of SNRs from comparison of the l-distribution of bright SNRs with various models. This includes comparison with the distribution from Case & Bhattacharya (1998), hereafter CB98 (see also Case & Bhattacharya 1996), which has been widely used. The conclusions are summarized in Section 4. Preliminary results have been presented in Green (2012, 2014b), but here a more detailed analysis is made.

2 GALACTIC SNRs

2.1 The catalogue of SNRs

I have produced several catalogues of Galactic SNRs, with published versions in Green (1984, 1988, 1991, 1996b, 2004, 2009, 2014a), and also various versions online since 1993.[1] Of the 294 remnants in the most recent version of the catalogue, most have been first identified at radio wavelengths, or – if identified at other wavebands – have subsequently been detected at radio wavelengths. But there are 22 remnants in the catalogue that have not yet been detected at radio wavelengths, or not sufficiently well observed to provide an integrated radio flux density. At optical and X-ray wavelengths only about 40 and 30 per cent, respectively, of the catalogued SNRs have been detected (which is not surprising, due to Galactic absorption that affects these wavelengths). Thus, it is selection effects at radio wavelengths that are dominant when considering the completeness of the catalogue. Fig. 1 shows a histogram of the date of inclusion of a remnant in the catalogue (the larger number of entries in the first version of the catalogue, from 1984, were largely taken from earlier Galactic SNR catalogues). This shows that major radio surveys have been the cause of significant increases in the identification of Galactic SNRs, notably:

★ E-mail: dag@mrao.cam.ac.uk

[1] See: http://www.mrao.cam.ac.uk/surveys/snrs/.

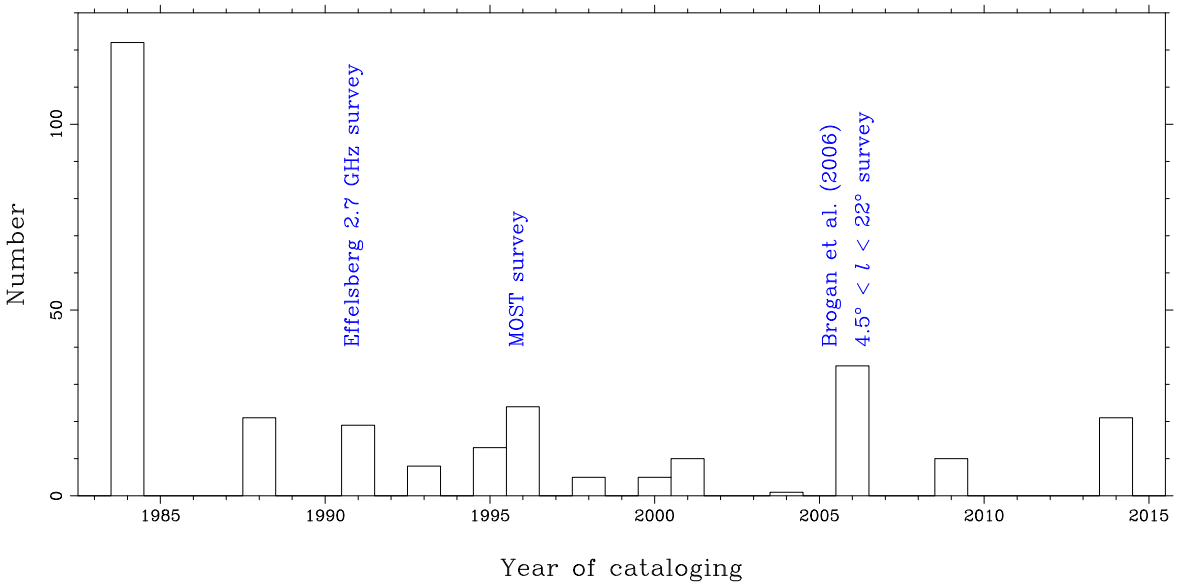

Figure 1. Histogram of the dates when Galactic SNRs were first catalogued.

(i) the Effelsberg 2.7-GHz survey (Fürst et al. 1990; Reich et al. 1990), covering $-2.6^\circ < l < 240^\circ$, $|b| < 5^\circ$, with a resolution of ≈4.3 arcmin;

(ii) the *MOST* 843-GHz survey (Green et al. 1999), covering $245^\circ < l < 255^\circ$, $|b| < 1.^\circ5$, with a resolution of ≈0.7 arcmin at best;

(iii) Brogan et al. (2006)'s survey of a small region of the 1st Galactic quadrant – $4.^\circ5 < l < 22^\circ$, $|b| < 1.^\circ25$ – at multiple radio wavelengths, with a resolution of ≈0.6 arcmin at 327 MHz, which also used infrared observations to help discriminate between different types of sources.

In the latest revision of the Galactic SNR catalogue, 21 new remnants were added to the catalogue. Of these 13 have an integrated radio flux density at 1 GHz in the catalogue, and hence a surface brightness, Σ can be calculated; all of these 13 remnants are faint, with $\Sigma_{1\,\mathrm{GHz}} < 8 \times 10^{-21}$ W m^{-2} Hz^{-1} sr^{-1}. The other eight newly catalogued remnants do not yet have radio flux densities reported in the literature, as they were identified at optical or X-ray wavelengths (e.g. G38·7−1·3, G65·8−0·5, G66·0−0·0, G67·6−0·0, G67·6+0·9 and G67·8+0·5 were identified from optical observations by Sabin et al. 2013 – for these SNRs integrated radio flux densities have not been yet published).

In order to derive directly the distribution of SNRs in the Galaxy, both: (i) correction for the incompleteness of the current catalogue of SNRs due to observational selection effects, and (ii) knowledge of the distances to each known SNR is required. I discuss below the selection effects that apply, at radio wavelengths, to the current SNR catalogue, and also some issues with the derivation of distances to individual SNRs using the 'Σ–D' relation.

2.2 Selection effects

As noted above, most Galactic SNRs are identified at radio wavelengths, and the selection effects that apply – as discussed previously, e.g. Green (1991, 2005) – are (i) intrinsically faint remnants (i.e. low surface brightness) are difficult to identify, and (ii) physically small but distant remnants are difficult to recognize as SNRs, due to their small angular sizes.

I have previously argued (Green 2004) for a nominal surface brightness completeness limit of ≈10^{-20} W m^{-2} Hz^{-1} sr^{-1}. (which is equivalent to ≈65 mJy per 1 arcmin circular beam). However, a higher limit probably applies close to the Galactic Centre (GC), where the background Galactic radio emission is brighter than elsewhere. The validity of this value for the approximate surface brightness completeness of the current SNR catalogue is discussed further below.

In addition to the difficulty of identifying low surface brightness SNRs, it is also difficult to identify small angular size remnants. For example, the Effelsberg 2.7-GHz survey has a resolution of 4.3 arcmin, and SNRs would have to be several times this angular size for their structure to be recognized. Reich et al. (1988) reported 32 new SNRs in the first part of the area covered by the Effelsberg 2.7-GHz survey ($-2.^\circ6 \le l \le 76^\circ$, $|b| \le 5^\circ$, subsequently published in Reich et al. 1990). Of these 30 are resolved, with angular diameters of 16 arcmin or more, i.e. several times the resolution of the survey. The other two sources have small angular size, and were thought to be SNRs on the basis of other, higher resolution targeted observations: (i) G54·1+0·3, then thought to be a small, ≈1.5 arcmin 'filled centre' remnant (see Green 1985; Reich et al. 1985), but is now catalogued as a slightly larger ≈12 arcmin composite remnant, since a faint X-ray halo was detected by Bocchino, Bandiera & Gelfand (2010), and (ii) G70·7+1·2, which was reported as an SNR by Reich et al. (1985), but this identification was not supported by subsequent observations (e.g. Green 1986; Onello et al. 1995; Cameron & Kulkarni 2007 and references therein). Given that SNRs are expected to have a continuous range of physical diameters, and are seen at a range of distances in the Galaxy, then a smooth distribution of angular sizes is expected. Fig. 2 shows a histogram of the angular size, θ, of catalogued SNRs, which clearly shows a sharp decrease at small angular sizes (<4 arcmin), due to the difficulty in identifying small SNRs.

Although there are some small angular size remnants in the catalogue identified from high resolution observations – notably G1·9+0·3 (e.g. Green et al. 2008; Reynolds et al. 2008; Borkowski et al. 2014), with an angular diameter of only 1.5 arcmin, many are missing. These missing young but distant SNRs will be on the far side of the Galaxy, and hence concentrated towards $l = 0^\circ$, $b = 0^\circ$,

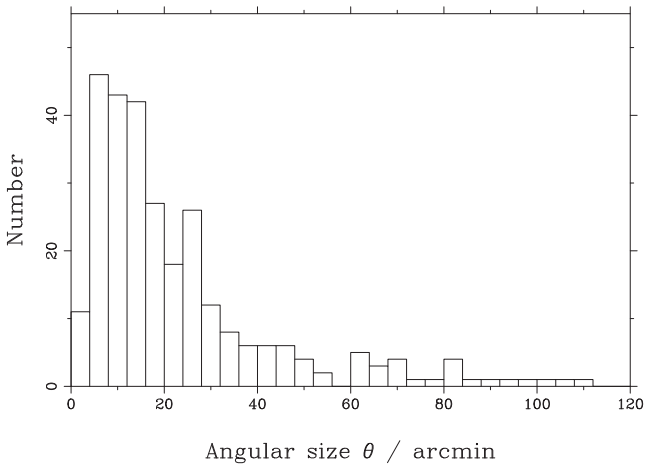

Figure 2. Histogram of the angular size, θ, of the catalogued Galactic SNRs (there are also 10 large remnants with angular sizes greater than 2° which are not included in this plot).

where confusion due to other Galactic sources along the line of sight makes their identification difficult.

To justify the nominal surface brightness completeness limit of $\approx 10^{-20}$ W m^{-2} Hz^{-1} sr^{-1} is appropriate, Fig. 3 shows histograms of: (a) 272 of the 294 catalogued SNRs which have an integrated flux density, and hence a surface brightness at 1 GHz; (b) 171 SNRs in the Effelsberg 2.7-GHz survey region; (c) 38 SNRs in the Effelsberg 2.7-GHz survey region entered into my SNR catalogue since 1992, i.e. those not identified from the Effelsberg 2.7-GHz survey.

Fig. 3(a) shows that the majority of SNRs identified are fainter than this nominal surface brightness limit, with 69 'bright' remnants above the limit. The fainter remnants are more easily detected in regions where the Galactic background emission is fainter, i.e. away from $b = 0°$ and $l = 0°$, which is illustrated in Figs 4 and 5. Fig. 4 shows the distribution in Galactic coordinates of (a) all remnants, and (b) the 69 'bright' remnants. The distribution of all remnants, without taking the surface brightness effect into account, is very much broader in both coordinates than that of the bright remnants (the rms deviations from the GC are 42° and 2°.4 in l and b, respectively for all SNRs, with 36° and 1°.3 for the 69 'bright' SNRs). Fig. 5 shows the surface brightness and Galactic longitude of the 272 catalogued SNRs with radio flux densities. In the Galactic anticentre (i.e. the second and third Galactic quadrants) – where the Galactic background is low – there is a higher proportion of low surface brightness SNRs.

Figs 3(b) and (c) show that the majority of SNRs identified in the Effelsberg 2.7-GHz survey region from subsequent other observations are fainter than the nominal surface brightness limit. However, there are six SNRs above the surface brightness limit, which have subsequently been identified, see Table 1 (some of these had been suggested as possible SNRs earlier). These six remnants are all close to the GC, or are small angular size, so would not have been well resolved in the Effelsberg 2.7-GHz survey, which is necessary to be recognized as an SNR.

A surface brightness completeness limit of $\Sigma_{1\,\mathrm{GHz}} \approx 10^{-20}$ W m^{-2} Hz^{-1} sr^{-1} is also consistent with observations made by Xu et al. (2013). Their observations covered $66° < l < 90°$, $|b| < 4°$ at 5 GHz, and they used other radio and infrared observations to separate non-thermal and thermal components. This multiwavelength approach should allow fainter remnants to be

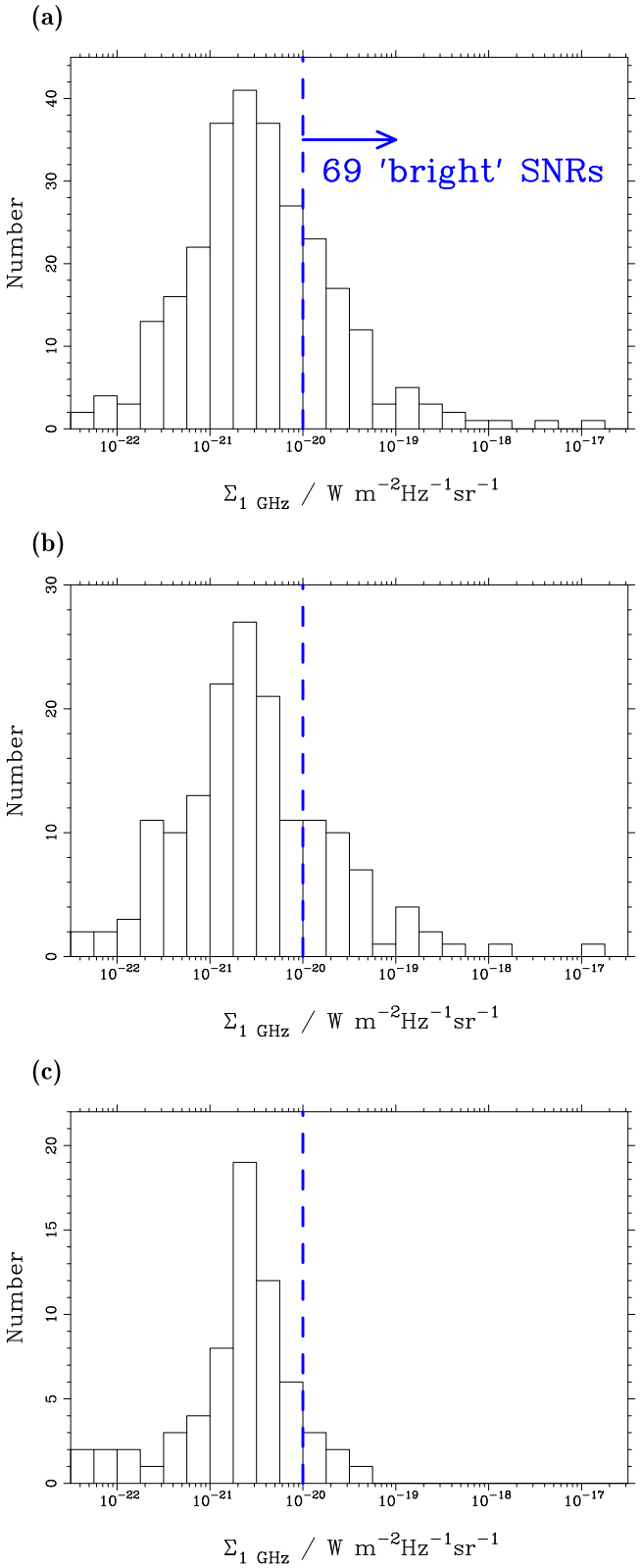

Figure 3. Histograms of surface brightness at 1 GHz for catalogued SNRs with a radio flux density at 1 GHz for: (a) SNRs; (b) SNRs in the region covered by the Effelsberg 2.7-GHz survey (i.e. $-2° < 240°$, $|b| < 5°$), (c) SNRs in the Effelsberg survey region identified since 1992.

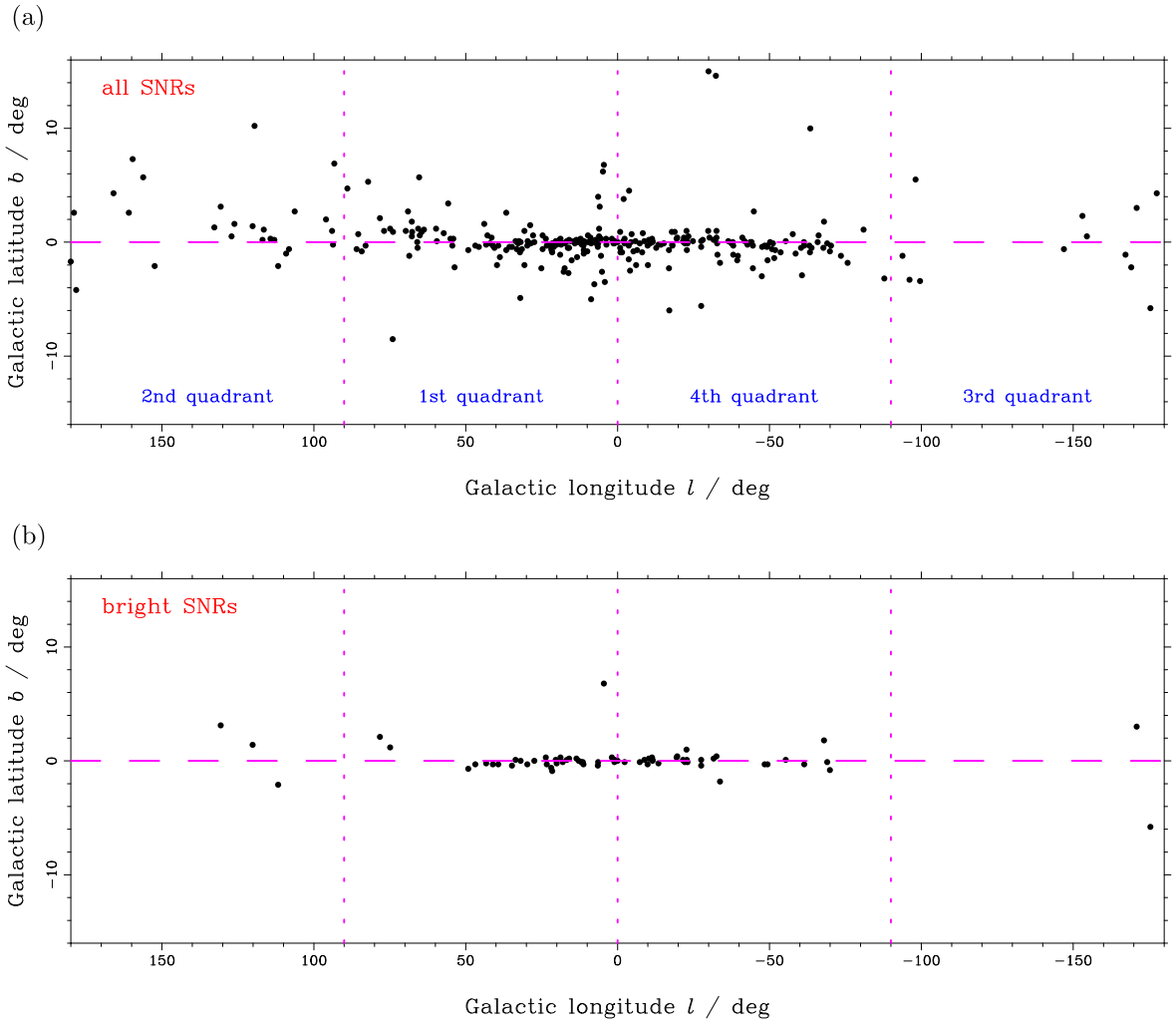

Figure 4. The distribution of SNRs in Galactic coordinates of all 294 catalogued SNRs for: (a) all SNRs, (b) the 69 'bright' SNRs with a surface brightness above 10^{-20} W m^{-2} Hz^{-1} sr^{-1}. Note that the latitude scale is exaggerated.

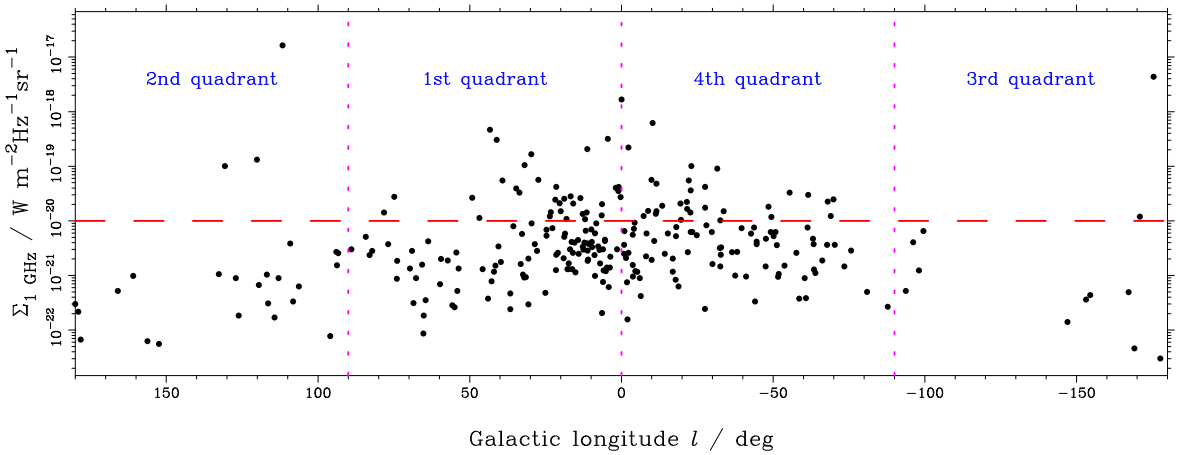

Figure 5. Radio surface brightness at 1 GHz against Galactic longitude for the 272 catalogued SNRs with radio flux densities. The nominal surface brightness limit of $\Sigma_{1\,\mathrm{GHz}} = 10^{-20}$ W m^{-2} Hz^{-1} sr^{-1} is shown.

recognized than is possible using a single observation frequency. They concluded that there were no large, i.e. sufficiently resolved, remnants with $\Sigma_{1\,\mathrm{GHz}} \gtrapprox 0.37 \times 10^{-20}$ W m^{-2} Hz^{-1} sr^{-1} in the region they observed.

Fig. 6 shows the distribution of SNRs with Galactic longitude. For all SNRs, Fig. 6(a) shows a clear asymmetry on different sides of $l = 0°$, with more SNRs identified in the first and second quadrants. This is because (i) the first and second quadrants are accessible to

Table 1. SNRs in Effelsberg 2.7-GHz survey region with $\Sigma_{1\,\mathrm{GHz}} > 10^{-20}$ W m^{-2} Hz^{-1} sr^{-1} identified since 1992.

Name	θ (arcmin)	$S_{1\,\mathrm{GHz}}$ (Jy)	$\log \Sigma_{1\,\mathrm{GHz}}$ (W m^{-2} Hz^{-1} sr^{-1})
G0·3+0·0	15 × 8	22	−19.56
G1·0−0·1	8	15	−19.45
G6·5−0·4	18	27	−19.90
G12·8−0·0	3	0.8	−19.87
G18·1−0·1	8	4.6	−19.97
G20·4+0·1	8	9.0	−19.67

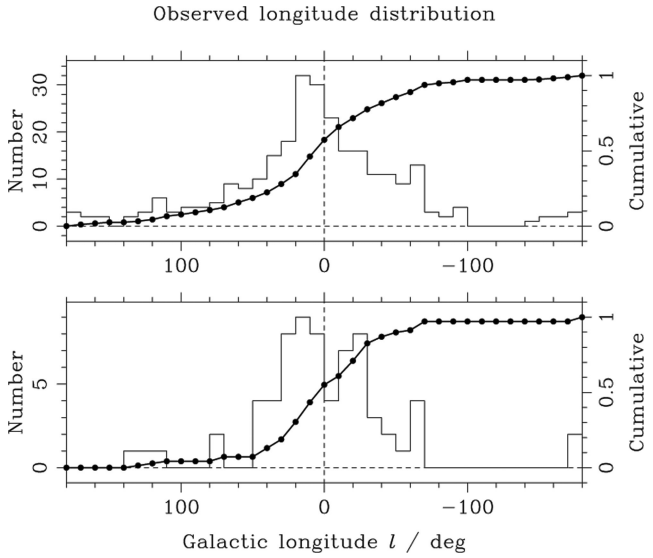

Figure 6. Histogram of the distribution of Galactic SNRs (left scale) and the cumulative fraction (right scale) with Galactic longitude, for (a) all 294 catalogued SNRs, and (b) the 69 'bright' SNRs.

a large number of Northern hemisphere telescopes, and (ii) they include the deep, multiwavelength survey of $4.^{\circ}5 < l < 22^{\circ}$, $|b| < 1.^{\circ}25$ by Brogan et al. (2006), as discussed in Section 2. The sample of 69 'bright' SNRs, Fig. 6(b), shows a much smaller asymmetry close to $l = 0^{\circ}$, but this is not statistically significant (four in the region $350^{\circ} \leq l < 0^{\circ}$, and eight – including G0·0+0·0 in the region $0^{\circ} \leq l < 10^{\circ}$). By Galactic quadrants, the numbers of bright SNRs are: 35 in the first, 3 in the second, 2 in the third, and 29 in the fourth. These, with Poisson errors, do not show any asymmetry between either side of the GC. This implies that the nominal completeness surface brightness cutoff, although derived from the Effelsberg 2.7-GHz – which misses almost all of the fourth quadrant – is applicable there. Fig. 6 again shows that the distribution of the 'bright' SNRs is more localized towards $l = 0^{\circ}$ than the distribution of all catalogued SNRs.

2.3 The 'Σ–D' relation

Although distance determinations are available for some Galactic SNRs – e.g. Pavlović et al. (2013) give a compilation of distances to 60 SNRs from the literature – the Σ–D relation has been used for some time (e.g. Ilovaisky & Lequeux 1972; Clark & Caswell 1976) to determine distances for other remnants. This is based on the fact that, for remnants with known distances, the observed surface brightness (Σ) is larger for SNRs with smaller physical diameters (D). This correlation is parametrized as

$$\Sigma = AD^{n}, \tag{1}$$

i.e. a straight line in the $\log D - \log \Sigma$ plane, with A and n determined from the properties of SNRs with known distances, The *observed* surface brightness, Σ – which is distance-independent – for a remnant without a distance determination can then be used to determine its physical diameter, D. Hence via its *observed* angular size, θ, its distance $d = D/\theta$ can be determined. However – as previously discussed (Green 1991, 2005) – there is a large scatter in the observed Σ–D distribution of SNRs, about an order of magnitude in D for a given Σ. In addition, small and/or faint SNRs are more likely to have been missed in current surveys, and be missing from the current Galactic SNR catalogue, due to the observational selection effects discussed in Section 2.2. So, the true range of diameters for a given surface brightness may extend to lower diameters. (On the other hand, for a given surface brightness, the upper limit to the range of diameters is not affected by selection effects, at least down to the nominal surface brightness limit of current catalogues.) Although the upper-right boundary of the observed Σ–D distribution of SNRs with known distances is useful to provide an upper limit on the diameter of an individual SNR, distances for individual SNRs derived from the Σ–D relation are imprecise.

Leaving aside issues with selection effects, if a Σ–D relation is to be used statistically to derive distances to individual SNRs from their surface brightness, care has to be taken to use the appropriate form of regression (Green 2005). Since the Σ–D relation is used to derive D from Σ then a regression that minimises square deviations in $\log D$ should be used, *not* a regression than minimises square deviations in $\log \Sigma$. For distributions with a large spread – as is the case for SNRs with known distances – different regressions give significantly different fits (see Isobe et al. 1990; Feigelson & Babu 1992 and Feigelson & Babu 2011 for discussion of different forms of least-square regressions).

CB98 derived a Σ–D relation with

$$\Sigma \propto D^{-2.64\pm0.26}, \tag{2}$$

using 37 Galactic 'shell' SNRs with known distances (or $\Sigma \propto D^{-2.38\,\pm\,0.26}$ if Cas A (=G111·7−2·1) is excluded). CB98 comment that these Σ–D slopes are significantly flatter than those derived in previous studies, e.g. Milne (1979) obtained $\Sigma \propto D^{-3.8}$. It is evident, however, that CB98 minimized square deviations in $\log \Sigma$, whereas Milne (1979) minimized square deviations in $\log D$, so these Σ–D slopes are not directly comparable. Re-fitting the SNRs with known distances used by CB98, minimizing deviations in $\log D$ rather than $\log \Sigma$ produces much steeper Σ–D slopes, which *are* in good agreement with earlier results (e.g. those of Milne). For all 37 'shell' SNRs

$$\Sigma \propto D^{-3.58\pm0.33}, \tag{3}$$

(or $\Sigma \propto D^{-3.37\,\pm\,0.35}$ if Cas A is excluded). This difference in the slope of the derived Σ–D relation depending on the form of regression used has an important consequence for the Galactic SNR distribution derived by CB98. There is a systematic bias in the diameters and hence distances derived for SNRs, with fainter/brighter SNRs having distances that are too large/small, respectively. Since there are more faint SNRs than bright SNRs, then the derived distribution of SNRs in the Galaxy will be systematically spread out too. In Σ–D studies in the literature, it is not always clear what form of regression was used. Re-analysing the published lists of SNRs with known distances implies that others (e.g. Göbel, Hirth & Fürst

1981; Huang & Thaddeus 1985; Arbutina & Urošević 2005; Stupar et al. 2007) have,[2] like CB98, used regressions which minimize deviations on log Σ rather than log D.

Pavlović et al. (2013) discussed the fitting of a Σ–D relation to Galactic SNRs with known distances, and concluded from Monte Carlo simulations that 'orthogonal regression' gives the best result. This conclusion is to be expected, given that in their Monte Carlo simulations Pavlovic et al. assumes 'scatter' in log D and log Σ of same magnitude, which is not realistic. In practice, the errors in surface brightness which depends on the uncertainties in flux density and angular size are likely to be smaller than the errors in distances (as Pavlovic et al. say in their introduction). When the errors in log D and log Σ are different, then the orthogonal fitting does not produce the correct result. Moreover, if the Σ–D relation is to be used to derive distances to individual SNRs, then a regression minimizing deviations in log D should be used to obtain the best result.

3 THE GALACTIC RADIAL DISTRIBUTION OF SNRs

Given the limitations of the Σ–D relation and the selection effects that apply to the identification of SNRs, rather than deriving the distribution of SNRs in the Galaxy directly – as done by CB98 – an alternative approach is to consider the l-distribution of sample SNRs. This can be compared with the expected l-distribution from various models.

Here I choose the sample of 69 'bright' SNRs, above the nominal surface brightness limit of $\Sigma_{1\,\mathrm{GHz}} = 10^{-20}\,\mathrm{W\,m^{-2}\,Hz^{-1}\,sr^{-1}}$, where the current catalogue of Galactic SNRs is thought to be nearly complete. This method has the advantage of avoiding all of the uncertainties from the Σ–D relation, but has the disadvantage of only using a fraction of the total number of catalogued Galactic SNRs. I include checks on how dependent the results are on a choice of surface brightness limit, or exclusion of regions close to $l = 0^\circ$. As noted above, a single surface brightness limit is not appropriate at all Galactic latitudes, and some SNRs above this nominal limit may well be missed in the brightest part of the Galactic plane, i.e. at latitudes near $l = 0^\circ$. Moreover, the difficulty of identifying small angular size remnants is also more of an issue nearer $l = 0^\circ$. Nevertheless, this sample is not as strongly affected by selection effects as the complete catalogue.

Here, I use a power-law/exponential model for the Galactic surface density of SNRs with Galactocentric radius, R, with

$$\propto \left(\frac{R}{R_\odot}\right)^{\alpha} \exp\left(-\beta\frac{(R-R_\odot)}{R_\odot}\right), \qquad (4)$$

where $R_\odot = 8.5$ kpc (i.e. a cylindrically symmetrical distribution about the GC). Given the limited number of SNRs in the sample of 'bright' remnants, no attempt is made here to constrain the form of the distribution perpendicular to the Galactic plane. This model for the surface density of SNRs tends to a zero density towards the GC, which better matches the distributions derived for pulsars and star formation in the Galaxy (e.g. Johnston 1994; Bronfman et al. 2000; Paladini, Davies & De Zotti 2004; Yusifov & Küçük 2004) than, for example, a simple Gaussian distribution (which I used in Green 1996a). This power law/exponential is one of the two models used

[2] This is contrary to the statement in Pavlović et al. (2013) that all previous Σ–D studies used regression minimizing deviations in log Σ.

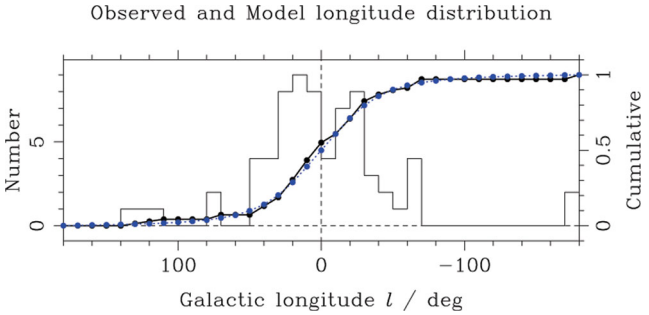

Figure 7. Histogram of the distribution of Galactic SNRs (left-hand scale) and the cumulative fraction – solid black line – (right-hand scale) with Galactic longitude for the 69 'bright' SNRs. The dotted blue line is the cumulative fraction for the best-fitting power-law/exponential model (with $\alpha = 1.09$ and $\beta = 3.87$).

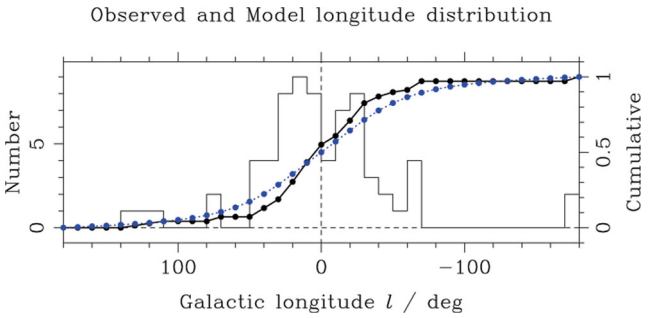

Figure 8. As Fig. 7, but the dotted blue line is the cumulative fraction for the best-fitting power-law/exponential model from CB98 (with $\alpha = 2.00$ and $\beta = 3.53$).

by CB98, who obtained best-fitting parameters of $\alpha = 2.00 \pm 0.67$, $\beta = 3.53 \pm 0.77$.

The best-fitting power-law/exponential model to the 69 bright remnants, is shown in Fig. 7, which has $\alpha = 1.09$ and $\beta = 3.87$. The statistic used for the fitting was the least sum of squares of the differences between the observed and model cumulative fractions, summed over all latitude bins, i.e. if the observed and model cumulative fractions are $f_\mathrm{o}(i)$ and $f_\mathrm{m}(i)$, respectively, for the ith bin, the minimum of $\sum_i (f_\mathrm{o} - f_\mathrm{m})^2$. (The fitting was made with a model distribution of one million SNRs, out to a Galactocentric radius of 50 kpc, using bins of 10° in l.) The sum of squares misfit for the $\alpha = 1.09$ and $\beta = 3.87$ best fitting model is 0.0127. Fig. 8 shows the power-law/exponential model derived by CB98, which is a poor fit to the observed distribution of the 69 bright SNRs, with a sum of squares misfit of 0.0841. This clearly represents a broader distribution (e.g. a flatter slope of the cumulative distribution near $l = 0^\circ$ than what is observed for the 'bright' remnants) than that shown in Fig. 7. This is not surprising given the systematic bias in the distances derived from the Σ–D relation used by CB98 which was noted in Section 2.3. The parameters for the best-fitting power-law/exponential model for the sample of 69 bright SNRs, and that from CB98 are shown in Table 2. The broader CB98 distribution is also evident in Fig. 9, which shows the surface density distribution of SNRs with Galactocentric radius for CB98's model, and the best fit to the 69 bright remnants. For CB98's best-fitting model, only 49 per cent of SNRs are inside the Solar Circle, compared with 73 per cent for the best fit to the 69 bright remnants.

The parameters of the best-fitting model are not well defined, as there is a strong degeneracy between the parameters, e.g. it is possible to obtain almost as good fits with, $\alpha = 2.00$, $\beta = 5.11$ or

Table 2. Best-fitting power-law/exponential models for different samples of Galactic SNRs, and other power-law/exponential models for comparison. (a) for the first four rows, the α and β values are for the best fit; (b) the fifth row uses the α and β best-fitting values from CB98; (c) the final two entries use one or other of the best-fitting values for α and β from CB98 and varies the other for a best fit.

	$\Sigma_{1\,\mathrm{GHz}}$ cutoff (W m^{-2} Hz^{-1} sr^{-1})	l-range	Number of SNRs	Fit parameters α	β	Proportion inside Solar Circle
Bright sample	10^{-20}	all	69	1.09	3.87	73 per cent
Brighter sample	2×10^{-20}	all	44	0.51	2.91	70 per cent
Fainter sample	5×10^{-21}	all	103	1.49	4.60	77 per cent
Omit near GC sample	10^{-20}	$\lvert l\rvert > 10^\circ$	57	0.0	2.76	77 per cent
CB98 best fit	10^{-20}	all	69	2.00	3.53	49 per cent
CB98 α fixed	10^{-20}	all	69	2.00	5.11	76 per cent
CB98 β fixed	10^{-20}	all	69	0.85	3.53	73 per cent

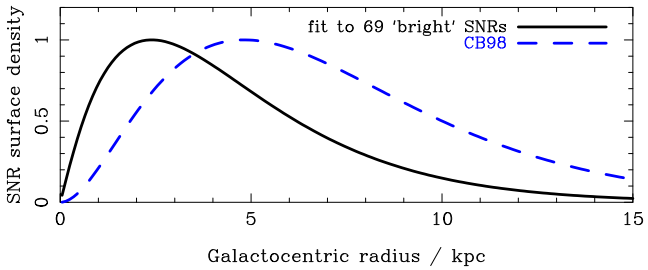

Figure 9. Normalized surface density of SNRs with Galactocentric radius for power-law/exponential models: (i) solid line, the best fit to l-distribution of 69 bright SNRs, and (ii) dashed line, from CB98.

$\alpha = 0.85$, $\beta = 3.53$ (i.e. fixing one parameter to the value obtained by CB98, and varying the other),which have sum of squares misfits of 0.0135 and 0.0128, respectively. The distribution with $\alpha = 2.00$, $\beta = 5.10$ peaks at a slightly larger radius from GC than the best-fitting distribution with $\alpha = 1.10$ and $\beta = 3.90$, but has a similar fraction of SNRs, 76 per cent, inside the Solar Circle. Conversely the distribution with $\alpha = 2.00$, $\beta = 5.10$ peaks closer to the GC, but again has a similar fraction of SNRs, 73 per cent, inside the Solar Circle.

Also, the best-fitting model depends on (i) the accuracy of the value of the surface brightness cutoff chosen to define the sample of 'bright' SNRs, and also (ii) the assumption that the remaining selection effects, which are more important close to $l = 0^\circ$ are not important. To investigate these, I have done the analysis with different $\Sigma_{1\,\mathrm{GHz}}$ cutoff values (lower and higher by a factor of 2), and excluding SNRs within 10° of $l = 0^\circ$. Varying the surface brightness by a factor of 2 – the 'brighter' and 'fainter' samples in Table 2 – does give rather different parameters, and hence different radial distribution, but the fraction of SNRs within the Solar Circle does not change strongly. When the region $|l| \leq 10^\circ$ is excluded – the 'Omit near GC' sample in Table 2 – the best-fitting model is a pure exponential (but note that this fitting does not depend on $R \lesssim 1.5$ kpc). This suggests there are indeed residual selection effects near $l = 0^\circ$. Nevertheless, the main result, that the distribution obtained by CB98 is too broad compared with bright SNRs still holds. The conclusion is strengthened by the fact that any remaining incompleteness of the sample of 69 bright SNRs will concentrate towards $l = 0^\circ$.

Finally, it should be noted that the constraints presented here apply to the distribution of observed SNRs. If the observability of SNRs above the radio surface brightness limit depends on a property – e.g. ambient density – which varies with Galactocentric radius, then this will mean the distribution of SNRs is not the same as their parent SNe.

4 CONCLUSIONS

Here I have discussed some of the properties of the most recent catalogue of Galactic SNRs, which contains 294, particularly (i) the selection effects that apply to the completeness of the catalogue, and (ii) issues with using the 'Σ–D' relation to derive distances to individual remnants. By comparison of the distribution in Galactic longitude of a sample of 69 'bright' SNRs – which are not strongly affected by selection effects – with that expected from models, constraints are placed on the distribution of the SNRs with Galactocentric radius (using a power-law/exponential model). It is shown that the widely used distribution derived by CB98 is too broad.

ACKNOWLEDGEMENTS

I thank various colleagues for useful comments on this work. I am grateful to the National Centre for Radio Astrophysics of the Tata Institute of Fundamental Research, Pune for their hospitality during a recent visit, during which the work for this paper was completed.

REFERENCES

Arbutina B., Urošević D., 2005, MNRAS, 360, 76
Bell A. R., 2014, Braz. J. Phys., 44, 415
Bocchino F., Bandiera R., Gelfand J., 2010, A&A, 520, A71
Borkowski K. J., Reynolds S. P., Green D. A., Hwang U., Petre R., Krishnamurthy K., Willett R., 2014, ApJ, 790, L18
Brogan C. L., Gelfand J. D., Gaensler B. M., Kassim N. E., Lazio T. J. W., 2006, ApJ, 639, L25
Bronfman L., Casassus S., May J., Nyman L.-Å., 2000, A&A, 358, 521
Calore F., Cholis I., Weniger C., 2015, J. Cosmol. Astropart. Phys., 3, 038
Cameron P. B., Kulkarni S. R., 2007, ApJ, 665, L135
Case G., Bhattacharya D., 1996, A&AS, 120, 437
Case G. L., Bhattacharya D., 1998, ApJ, 504, 761 (CB98)
Clark D. H., Caswell J. L., 1976, MNRAS, 174, 267
Feigelson E. D., Babu G. J., 1992, ApJ, 397, 55
Feigelson E. D., Babu G. J., 2011, ApJ, 728, 72
Fürst E., Reich W., Reich P., Reif K., 1990, A&AS, 85, 691
Göbel W., Hirth W., Fürst E., 1981, A&A, 93, 43
Green D. A., 1984, MNRAS, 209, 449
Green D. A., 1985, MNRAS, 216, 691
Green D. A., 1986, MNRAS, 219, 39P
Green D. A., 1988, Ap&SS, 148, 3
Green D. A., 1991, PASP, 103, 209

Green D. A., 1996a, in McCray R., Wang Z., eds, Proc. IAU Colloq. 145, Supernovae and Supernova Remnants. Cambridge Univ. Press, Cambridge, p. 341
Green D. A., 1996b, in McCray R., Wang Z., eds, Proc. IAU Colloq. 145, Supernovae and Supernova Remnants, Cambridge Univ. Press, Cambridge, p. 419
Green D. A., 2004, Bull. Astron. Soc. India, 32, 335
Green D. A., 2005, Mem. Soc. Astron. Ital., 76, 534
Green D. A., 2009, Bull. Astron. Soc. India, 37, 45
Green D. A., 2012, in Aharonian F. A., Hofmann W., Rieger F. M., eds, AIP Conf. Proc. Vol. 1505, High Energy Gamma-ray Astronomy. Am. Inst. Phys., New York, p. 5
Green D. A., 2014a, Bull. Astron. Soc. India, 42, 47
Green D. A., 2014b, in Ray A., McCray R. A., eds, Proc. IAU Symp. 296, Supernova Environmental Impacts. Cambridge Univ. Press, Cambridge, p. 188
Green A. J., Cram L. E., Large M. I., Ye T., 1999, ApJS, 122, 207
Green D. A., Reynolds S. P., Borkowski K. J., Hwang U., Harrus I., Petre R., 2008, MNRAS, 387, L54
Huang Y.-L., Thaddeus P., 1985, ApJ, 295, L13
Ilovaisky S. A., Lequeux J., 1972, A&A, 18, 169
Isobe T., Feigelson E. D., Akritas M. G., Babu G. J., 1990, ApJ, 364, 104
Johnston S., 1994, MNRAS, 268, 595
Kumar R., Eichler D., 2014, ApJ, 785, 129
Lee S.-H. et al., 2011, Astropart. Phys, 35, 211
Li W., Chornock R., Leaman J., Filippenko A. V., Poznanski D., Wang X., Ganeshalingam M., Mannucci F., 2011, MNRAS, 412, 1473
Milne D. K., 1979, Aust. J. Phys., 32, 83
Onello J. S., Depree C. G., Phillips J. A., Goss W. M., 1995, ApJ, 449, L127
Paladini R., Davies R., De Zotti G., 2004, Ap&SS, 289, 363
Pavlović M. Z., Urošević D., Vukotić B., Arbutina B., Göker Ü. D., 2013, ApJS, 204, 4
Reich W., Fürst E., Altenhoff W. J., Reich P., Junkes N., 1985, A&A, 151, L10
Reich W., Fürst E., Reich P., Junkes N., 1988, in Roger R. S., Landecker T. L., eds, Proc. IAU Colloq. 101, Supernova Remnants and the Interstellar Medium. Cambridge Univ. Press, Cambridge, p. 293
Reich W., Fürst E., Reich P., Reif K., 1990, A&AS, 85, 633
Reynolds S. P., Borkowski K. J., Green D. A., Hwang U., Harrus I., Petre R., 2008, ApJ, 680, L41
Sabin L. et al., 2013, MNRAS, 431, 279
Stupar M., Filipović M. D., Parker Q. A., White G. L., Pannuti T. G., Jones P. A., 2007, Ap&SS, 307, 423
Vladimirov A. E., Jóhannesson G., Moskalenko I. V., Porter T. A., 2012, ApJ, 752, 68
Xu W. F., Gao X. Y., Han J. L., Liu F. S., 2013, A&A, 559, A81
Yusifov I., Küçük I., 2004, A&A, 422, 545

This paper has been typeset from a TEX/LATEX file prepared by the author.